

FACILITY FORM 602	(ACCESSION NUMBER)	(THRU)
	19	63
	(PAGES)	(CODE)
	CR-117141	29
	(NASA CR OR TMX OR AD NUMBER)	(CATEGORY)

Paper No. 19

SOLAR WIND SIMULATOR²H. J. King¹

REFERENCE: King, H. J., "Solar Wind Simulator," ASTM/IES/AIAA Space Simulation Conference, 14-16 September 1970.

ABSTRACT: It is necessary to expose samples of thermal control coating materials to a proton flux in the laboratory in order to estimate the stability of their reflective and absorptive properties when exposed to the solar wind. The choice of the ion source, mass separator, and beam transport system which make up an experimental apparatus to perform these tests is discussed. A final system design is presented which is capable of irradiating 10 standard samples 2 cm in diameter with a proton beam ranging in energy from 0.5 to 3.0 KeV and in intensity from 1 to 1000 times that of the nominal solar wind.

KEY WORDS: solar wind simulator, proton source, mass separator, ion optics, ion beam deflection

INTRODUCTION

Scientific probes traveling through space encounter several types of particle fluxes. A primary class are those emanating the sun—the so-called solar wind. A companion paper (1)³ describes these particles, their intensity and their relation to the activity cycle on the sun. This paper deals with the design of apparatus to simulate the solar wind in laboratory facilities.

¹Head, Propulsion Technology Section, Hughes Aircraft Research Laboratories, Malibu, California.

²This paper is based on NASA CR 73443 prepared for the Ames Research Center under contract NAS 2-5585. Please see the final report under this contract for a quantitative discussion of the material presented here.

³The numbers in parentheses refer to the list of references appended to this paper.

The solar wind simulator discussed herein is intended to be used for evaluating the synergistic effects of the combined particulate and photon radiation on thermal control coatings. Zuccaro (1) has discussed the basic requirements for apparatus to reliably evaluate these materials and the techniques to perform the experiments. This paper presents the design rationale behind the selection of the major components of the simulator.

SYSTEM DESIGN

The design of the apparatus such as shown in Fig. 1 requires the selection and design of the ion sources, the mass separator, and the beam transport system. The system must be capable of irradiating 10 standard samples 2 cm in diameter with a proton beam ranging in intensity from 1 to 10^3 times that of the nominal solar wind. The nominal solar wind is defined as a pure proton flux of 2×10^8 protons/cm²-sec (3.2×10^{-11} A/cm²) ranging in energy from 0.5 to 3.0 KeV with a nominal mean energy of 1.0 KeV.

A. ION SOURCES

1. Physical Characteristics

The characteristics of the ion source affect all the other major components of the system — the ion optics, the mass separator, and the vacuum station itself. Fortunately, for this study, proton sources have played an important role in nuclear physics for many years, so that a large body of information is available to define and compare the various possible source configurations. Before considering individual ion sources in detail, it is appropriate to interpret the previous section in terms of the conditions which it imposes on the ion source.

Considering the nominal intensity of the solar wind, the desire to accelerate the test time by a factor of 1000, the target size and attenuation in the apparatus, the ion source must generate a proton current of approximately 10^{-5} A. The bulk of the protons in the solar wind range in energy from 0.5 to 3.0 kV. In order to provide the necessary experimental flexibility, the apparatus must be designed so that the proton energy is variable, at least over this range. While it is well within the capability of the designer to make the instantaneous ion energy a variable, this should not be confused with the virtually impossible task of providing an ion beam which contains a controllable mixture of all ion energies at a given time. Fortunately, the latter is not required for an accurate simulation of solar wind.

A related characteristic is the energy spectrum of the ions inside the ion source. This energy spread appears as an uncertainty in the final proton energy at the target. While this may not be detrimental to the experiment itself, it does impose severe limitations on the design of the ion beam transport and separation systems. Therefore, an ion source with a small energy spread is desirable.

Mass efficiency n_m is used to define the percentage of hydrogen atoms that actually leave the source as protons. A high mass efficiency is desirable to reduce the neutral density in the region immediately downstream of the source. This reduces the creation of charge exchange ions which contaminate the beam. (See Ref. 1)

The useful lifetime of the source is important for an apparatus in which experimental simulation may be conducted in real time. The arbitrary, but realistic, lifetime goal set for this design was 1000 hours (~6 weeks).

The above characteristics provide a scale against which the various sources may be compared. Where possible this comparison is made quantitatively in Table 1.

2. Types of Proton Sources

There are a large number of generic types of ion sources, each with many individual designs, which will produce a proton beam. An excellent review of the basic types was presented by Hoyaux and Dujardin (2). All of these sources dissociate and ionize the hydrogen by electron bombardment. They differ radically in power requirements and general operating conditions. Of particular interest for this application are two requirements mentioned earlier; namely, a minimum kinetic ion energy spread in the source and the ability to vary the source output current intensity over a wide range to accommodate the required flux variations.

a. Radio Frequency Ion Sources (See Ref. 3)

The radio frequency ion source, sometimes called an electrodeless discharge source, has been a standard for many years in high voltage particle accelerators used for nuclear physics experiments. RF power is coupled into a quartz (or other insulating material) tube containing hydrogen gas at a pressure ranging from 10 to 100 μm of mercury. The mean free path of an electron in the source is on the order of 1 cm. Thus, electrons will be accelerated by the imposed electromagnetic field and will, under the proper conditions, generate a stable plasma from which an ion beam may be extracted.

The most common method of coupling rf power into the discharge is to place the discharge chamber inside a solenoid which is activated with rf power at approximately 10 MHz. The alternating magnetic field generated in the discharge chamber accelerates the electrons. Generally, the induced electric fields are relatively small here and the circulating currents rather large. Energy spreads ranging upward from 20 eV have typically been reported (4, 5) for this device. Quite frequently an axial magnetic field is used to increase the electron path length and to improve stability.

Beam currents up to 1 mA are typically reported for this type of source. Proton fractions up to 90% of the total ion current in the beam have been observed under optimum conditions; 50 to 70% is common for well designed sources. Hydrogen consumption varies according to source design but is typically of the order of 4 cm³/hour at STP for 1 mA of output beam. It may not be possible to scale down the gas flow directly with beam current. Operating frequency varies as well, ranging from 1 to 400 MHz; 10 MHz is common and rf power requirements are a few hundred watts. Source lifetimes of 1000 hours at the current levels required for this application are reported (6).

Of the various sources surveyed, the electromagnetic rf ion source most nearly meets all the requirements. It fully meets the beam requirements and is adequate in terms of mass efficiency and proton yield. If this type of source is to be designed or adapted to this application, care should be taken to assure stable operation over long periods by choosing high quality materials for its construction and designing both the power supplies and the hydrogen feed system with stability as a primary consideration.

b. Electron Bombardment Sources

As the name implies, electron bombardment sources ionize by direct impact of electrons on the hydrogen molecule or atom. The distinction here is that in contrast to other types of sources conditions are such that no plasma is created nor is any arc or discharge struck. While several designs are possible only the low voltage source is of interest here. Typical of the type most useful for the purpose at hand is that described by Redhead (7). Hydrogen gas is introduced into the ionization region where it is bombarded by electrons with the resulting production of protons. An axial magnetic field significantly increases the electron path length and hence the source efficiency. The electrons may be axially restrained by holding both ends of the discharge chamber at cathode potential, thus making it energetically impossible for electrons to reach them after any energy loss. Redhead has reported that this type of source is capable of trapping ions in the source for

periods as long as 1 sec. This is desirable in a proton source because when a proton collides with the metal wall of the source, it is re-emitted as part of a hydrogen molecule and must be both dissociated and ionized again to be useful.

This type of ion source has several advantages. Primary among these is that it fulfills the two desirable criteria mentioned earlier. It is adjustable in current over several orders of magnitude and produces ions with a relatively small energy spread, ranging down to less than 1 eV for specially designed sources⁽⁸⁾. The primary difficulty with this type of ion source is that the mass efficiency is of the order of 1% or less. Thus, it presents a large gas load to the system when operating at high output currents. A second, and less important, disadvantage is that the source requires a thermionic cathode, which is subject to contamination and has a finite lifetime.

A simple source of this type is in use at Hughes Aircraft Company⁽⁹⁾. It is capable of producing a proton current equivalent to 2000 times the nominal solar wind value over a 2.5 cm diameter circle. Input power is about 20 W. The entire vacuum station, including the source chamber and the integrating sphere, is pumped by a single 400 liter/sec ion pump. A single feedback loop that monitors the emitted ion beam current and adjusts the cathode emission to compensate for drift in line voltage or hydrogen flowrate serves to stabilize the beam for periods of several days.

c. Other Proton Sources

All other ion sources investigated were considered unsuitable for this application for a variety of reasons. These types included the high voltage and crossed field electron bombardment sources mentioned above, gas discharge sources such as the Penning or Finkelstein source, the duoplasmatron and the capillary arc. The reasons for this selection have been discussed in detail in the final report from which this paper was taken⁽¹⁰⁾ and are summarized in Table 1.

3. Ion Extraction Systems

The foregoing sections have discussed a number of proton sources. To be useful, these protons must be extracted from the source and focused into a beam. The ion extraction system which accomplishes this forms a critical interface between the source and the ion transport system which controls the beam shape en route to the target.

The theory of charged particle focusing has been investigated extensively in the development of electron guns used for many purposes. Because the focal properties of electrostatic

lenses are independent of particle mass, the theories derived for electrons are equally valid for protons. The principal difference is that the currents that may be carried with a given set of lenses and accelerating voltages are much less for protons than for electrons because the particle velocities for a given accelerating voltage vary inversely as the square root of the mass

The simple, but important, concept of operating the extraction system in an accel : decel mode is often overlooked by those designing ion transport systems. The ions are extracted with a total voltage greater than the desired beam voltage and then decelerated. This accomplishes two things. First, it prevents electrons from the beam or target from entering the source and damaging components or disturbing the control system which often operates on total emitted current. Second, it separates the extraction voltage from the beam voltage and permits a higher beam current to be extracted than would be possible at the beam voltage alone. It also permits adjustment of the beam voltage without disturbing the position of the plasma sheath because the total voltage may be held constant as the ion beam voltage is varied.

B. MASS SEPARATORS

All of the ion sources discussed above produce an ion beam output which is a mixture of protons, H_2^+ , H_3^+ , and many other ions. The sources may also produce a high flux of fast neutral particles by charge exchange and a number of ultraviolet photons which can degrade the test sample. The photons can create photo electrons if they are allowed to strike the target or the Faraday cup which monitors the beam. The mass separator, which is located between the proton source and the target, must purify the beam which passes through it so that only the protons will strike the target.

The physical separation of the protons from the rest of the beam can be accomplished in two basically different manners. An appreciation of the two concepts plays an important role in choosing the most desirable type of mass separator. All ion sources produce a mixture of protons, other positive ions, fast and slow neutral particles, photons from the discharge within the source and sputtered material from the ion extraction system or focusing lenses. The first method is to design a separator which selects only the protons from this beam. The trajectories of the protons are controlled so that they alone reach the target, which is shielded from the source so that none of the contaminants may reach it by line of sight. The magnetic sector magnet is an example of such a device. The second system concept is to provide a series of filters to prevent the unwanted particles from reaching the target while

permitting the desirable proton beam to pass. The difficulty here is first to identify all of the contaminants which may exist in the beam and then to devise filters which will selectively stop the contaminants but transmit the protons. This is particularly difficult in the case of photons and fast neutrals. The rf separator is an example of this type of system. As will be shown, a separator which deflects the proton beam is clearly superior for this application.

1. Physical Characteristics

The various separators were compared on the basis of their ability to produce a pure proton beam; transmit a large fraction of the incident photons; provide a continuous rather than pulsed beam; introduce minimum aberrations into the ion beam transport system; provide continuous, stable operation; accommodate a full range of ion velocities; and their ease of design and use.

2. Types of Mass Separators

Three general types of mass separators were considered:

- Radio Frequency - which utilizes resonance between particle inertia and an alternating electromagnetic field.
- Homogeneous Magnetic Field - in which the ions of different mass are spatially separated due to their different radius of curvature in a magnetic field.
- Crossed Field or ExB - where perpendicular static electric and magnetic fields cause different trajectories for different masses.

a. Radio Frequency

The basic concept of a linear rf mass spectrometer was first described by Bennett.⁽¹¹⁾ The operation had been analyzed by a number of authors, particularly Redhead and Crowell⁽¹⁷⁾, who list all the critical performance parameters for both sinusoidal and square wave operation.

The experimental performance for a system of this design has been reported recently (Ref. 13). This device has 13 grids, three rf stages, and two drift spaces. The complete system is 25 cm long and operates at 10 MHz. Assuming that each grid is 95% transparent but that the individual wires are randomly oriented with respect to those of the other grids, approximately 50% of the particles from the source will impinge on the grids. While the beam may be purified by this device to greater than

95%, it can be accomplished only at the expense of reducing the transmission to less than 10%. This in itself may be quite tolerable if a source with a sufficiently high output current is used. The difficulty arises because the photon output from the source and the beam of fast charge exchange neutrals created at the source aperture are not attenuated by the electric fields. Thus they are increased in relation to the proton beam by at least an order of magnitude using this type of separator. The effects of these contaminants may thus easily be greater than those of the proton beam for many operating conditions. A further complication is that the impurity beam may not be uniform over the target area and may be very difficult to measure accurately.

Therefore, even though this system has many advantages in terms of minimum energy dispersion, astigmatism, cost, and size, it is suggested that serious consideration be given to the problem of beam contamination before it can be used for any simulation.

b. Homogeneous Magnetic Field

This is a "conventional" type of mass separator which operates on the principle that the trajectory of a charged particle will be deflected by a magnetic field. A great deal of developmental work devoted to understanding and improving this type of mass spectrometer has been reviewed by Inghram and Hayden (14).

Of Primary importance to the overall system performance are two parameters of the separator design. The first is the angle through which the beam of interest (protons) is deflected. It is directly related to the strength of the magnetic field and the path length in the field. The second factor is the dispersion of the various masses at the target. In order to preserve the minimum beam size, the dispersion through the separator should be minimized. This may be done by establishing the minimum sector angle for the separator which will spatially separate the proton beam from the H_2^+ beam.

The magnetic sector mass separator is well suited for this task, provided that the beam is kept small in diameter until after separation and then expanded to cover the target area. The power requirements increase rapidly as the beam size increases, because of the resultant increase in magnetic gap. The magnetic fringing fields also become very difficult to adjust at large gap spacings, thus introducing unwanted aberrations in the final beam. This type of separator accomplishes the two necessary functions of bending the proton beam to physically remove it from the efflux of photons and neutrals from the ion source (which travel line of sight), and of dispersing the charge particles of various masses so that a pure

proton beam results. Care must be taken in the design to reduce the ion optical aberrations and to minimize the dispersion due to the energy distribution in the ion source.

c. Crossed Field or ExB

In a crossed field separator, the magnetic field B , the electric field E , and the velocity of a charged particle are all mutually perpendicular. If the signs are properly chosen, it is clear that by adjusting the magnitudes of the electric and magnetic field strengths the electric and magnetic forces on the particle may be made equal and opposite and the particle trajectory will be unchanged. Particles with the same kinetic energies but a different mass will follow a curved trajectory. The properties of this type of separator have been discussed by Bleakney and Hipple (15). The simplified analysis of Wahlin (16) is recommended as clearly illustrating the important processes. This type of separator will serve equally as well as the simple magnetic sector in many cases. The extra variable of the electric field strength provides the opportunity to design the system to achieve first order focusing.

3. Selection of the Mass Separator

The properties of the three types of mass separators discussed above are summarized in Table 2. Of the three, only the rf separator is clearly rejected because it does not prevent uncharged particles and photons from striking the target. The remaining two—the sector and crossed field separators—are similar in many respects. The crossed field separator contains aberrations from nonuniformities in both the electric and magnetic fields, while only a magnetic field is present in the sector. In particular, it is difficult to generate a uniform electric field when the magnetic and electric pole pieces of the crossed field separator must of necessity be in close proximity. This problem has recently been solved analytically and appears manageable for low energy applications such as that required for the present program.

The sector magnet was chosen over the crossed field device for the system design here, principally because it requires one less power supply and is a well understood, proven device. Techniques have been derived to produce very sophisticated instruments of this type, if they are required. Special attention should be devoted to the defocusing of the beam due to energy dispersion in the source. Careful design of both source and separator can keep this well within tolerable limits.

C. BEAM TRANSPORT SYSTEM

1. Introduction

The beam transport system must accept the ion beam from the source, focus it through the mass separator, and expand it to 10 cm diameter at the target plane. It must also be capable of providing adjustment of beam intensity by a factor of 1000. Finally, it must perform satisfactorily over the full range of proton energies from 0.5 to 3.0 kV. Two general concepts are possible. The first is to extract from the source a small, relatively high current density beam which is expanded in size only after it has passed through the mass separator. This considerably simplifies the design of the einzel lens, because all the beam ions pass through the lens near the axis where aberrations are small and the paraxial ray equation is valid. The mass separator is simplified as well because the magnet gap widths can be minimized. The single small aperture in the source serves to minimize the effluent hydrogen gas and the pumping speed necessary to maintain satisfactory chamber pressure. Finally, the small beam permits a series of apertures to be installed between the source and the main vacuum chamber, to reduce the diffusion of hydrogen from the source into the chamber. A separate pump is provided near the source.

The second approach is to extract a large beam from the source and transport this broad beam through the mass separator to the target. This virtually eliminates the need for an ion optical system, but entails a number of other difficulties which are obvious from the preceding paragraph. The only mass separator which readily accommodates a broad beam is the rf separator, although large aperture crossed field and even magnetic sector separators are possible at the low beam energies used here. Only the first type of system (i. e., small beam) will be treated here.

2. Computer Simulation of Ion Trajectories

As the name implies, each element in the ion optical system may be treated mathematically by techniques used in conventional geometrical optics. For instance, the einzel lenses have an equivalent thick lens analogy, and a sector magnet is equivalent to a cylindrical lens bounded on the entrance and exit sides by thin lenses. The focal properties of the lenses are a complicated function of the geometry, beam voltage, and lens voltage for each.

It has been shown (17) that where the paraxial ray equation is applicable, this problem may be readily treated by a matrix technique which is easily adaptable to computer calculation. Assuming circular symmetry, the trajectory of a particle may

be defined at any time by its radial distance and radial momentum and represented by a column vector. The effect of each ion optical element on the trajectory is represented by a two-by-two matrix so that the total transfer matrix for the entire system is thus a product of n matrices, where n is the number of ion optical elements in the system. It is clear that this formulation is suitable for computer calculation.

Only electrostatic lenses are considered here because they consume no power and are independent of the mass of the particle being focused. The most versatile type is the einzel lens which is composed of three apertures, or cylinders. The two end elements are connected together electrically so that the beam leaves the lens with the same kinetic energy with which it entered. The central element is biased to retard the beam (i. e., biased positively for positive ions). The focal length of the lens is a direct function of the ratio of the voltage on this central element to the beam voltage. While such lenses are simple in concept, they introduce sizable aberrations if the beam is not kept small relative to the lens aperture.

Three einzel lenses are used in the beam transport system for focusing purposes. The first, in conjunction with the weak focusing properties of the mass separator, focuses the beam through the aperture following the mass separator. This aperture also provides the pressure differential needed between the target and source chambers. The second lens produces a magnified image of the aperture, resulting in a 10 cm diameter image at the target. The third lens (optional) provides the slight collimation needed to produce an exactly parallel beam at the target. Without this last einzel lens the long "throw" of the second einzel produces a landing angle of $\tan^{-1} (5/100) \approx 2.7$ deg.

Because of the large number of elements in the system, the operation of the beam transport system is too complex to describe quantitatively here. Interested readers are referred to the final report on NASA Contract NAS 2-5585 (10) for a detailed description.

The total system must be able to change the target current by three orders of magnitude. Because it is not possible to operate the rf source over such a wide dynamic range, it is necessary that the beam transport system provide approximately a factor of 100 intensity variation, which together with a variation of source current by a factor of 10 provides the total dynamic range required. The source current will be varied by changing the neutral H_2 flow and/or the rf excitation power. The variation provided by the beam transport system is accomplished by flooding an aperture and allowing only a small fraction of the current to pass through the aperture by changing the

first einzel focusing voltage. This means the beam size at the aperture may be varied from a radius of less than 0.1 cm to greater than 1.1 cm by the first einzel. This is about the maximum intensity ratio possible with this method because the image size at the target is limited by the maximum magnification (minimum focal length) of the lens.

3. Beam Rastering System

The system illustrated in Fig. 2 is based on the requirement that the simulation requires a large dc proton beam which covers all of the target area uniformly. It has been estimated (10) that the simulation would not be impaired if the protons arrived at the target as a series of discrete pulses at rf frequencies. If it can be demonstrated experimentally that this is indeed true, a system employing a small diameter proton beam which is swept over the target surface is a pattern similar to the electron beam in a TV raster has many advantages. The system shown in Fig. 2 is easily converted to this design by changing the operating voltage of diverging einzel lens No. 2 to focus the beam to a spot on the target and introducing two pairs of orthogonal electrostatic deflecting plates in place of optional collimating einzel lens No. 3.

The advantages of a rastered system are

1. By sweeping a small beam over the large target area, the beam nonuniformities are smeared out and the coverage may be made as uniform as desired, even if some lens aberrations exist.
2. By programming the rate at which the beam is swept, the dose rate to each individual sample may be controlled (as a function of exposure time if desired).
3. The dose rate may be attenuated over several orders of magnitude while the source operates at the single fixed point where it performs best. This is achieved by deflecting the small beam off the target area entirely for some fraction of each raster period. This not only extends the operating range of the system, but simplifies the design of the ion source and its control system.
4. The accuracy of the dose measurement is improved by this technique because the total proton beam (which may be measured accurately) is projected onto each area of the target for a time, which also can be measured accurately. The result is a far more accurate measure of dose than sampling a small fraction of the beam and relying on a prior measurement of beam homogeneity.

It is also much easier to design a dynamic control system for this system than for one that samples a fraction ($\sim 1\%$) of the beam current (i. e., $\sim 10^{-11}$ A).

D. CONCLUSIONS

The discussion in the preceding section illustrates that a system of the general design shown in Fig. 1 can indeed be designed and that the requirements on each of the various components required is within the current state of the art. The most critical area requiring experimental verification and possibly further development is the design of the ion extraction system which draws protons from the source and focuses them into a parallel, laminar flow beam. This interface between proton source and the rest of the system is the key to successfully producing a beam of uniform current density at the target.

Two important design principles were formulated as a result of this study. The first is that the proton beam should be bent during its traversal of the system so that it is possible to completely shield the target from photons, fast neutrals and possibly sputtered material that are inadvertently produced by the source. The second design philosophy is that if it does not reduce the experimental accuracy it is more desirable from a system designer's viewpoint to irradiate the target with a small beam which is rastered over the surface than with a broad, uniform dilute beam.

References

1. Zuccaro, D. E., companion paper this conference.
2. Hoyaux, M. and Dujardin, I., *Nucleonics*, 4, 7; 4, 12; 5, 67 (1949).
3. Blanc, D. and Deghilh, A., *J. Phys. Radium* 22, 230 (1961).
4. Hall, R. N., *Rev. Sci. Instr.* 19, 905 (1948).
5. Thoneman, P. C., Moffatt, J., Roaf, D., and Sanders, J. H., *Proc. Roy. Soc.* 61, 483 (1948).
6. ORTEC Model 320 RF Ion Source Data Sheet.
7. Redhead, P. A., *Can. J. Phys.* 45, 1790 (1967).
8. Dworetzky, S. Novick, R. Smith, W. W. and Tolk, N., *Rev. Sci. Instr.* 39, 1721 (1968).
9. Constructed by H. J. King and D. E. Schnelker; unpublished.
10. Solar Wind Simulation Techniques Final Report Contract NAS 2-5585 HRL Staff (1970).

11. Bennett, W. H., J. Appl. Phys. 21, 143 (1950).
12. Redhead, P. A. and Crowell, C. R., J. Appl. Phys. 24, 331 (1953).
13. Lebduska, R. and Meckel, B., "Solar Wind Simulator and Advanced Design with Extended Operational Capabilities," AIAA Paper No. 70-31, January 1970.
14. Inghram, M. G. and Hayden, R. D., Handbook on Mass Spectroscopy (Nuclear Science Series, National Academy of Science, Washington, D.C., 1954), No. 14.
15. Bleakney, W. and Hipple, J., Phys. Rev. 53, 521 (1938).
16. Wahlin, L., Nucl. Instr. Methods 27, 55 (1967).
17. Cotte, M., Ann. Phys. (Paris) 10, 333 (1938).

Table 1--Ion Sources

Type of Source		Advantages	Disadvantages
Radio Frequency	Electromagnetic	Long life and high percent of protons	Narrow beam current range
	Electrostatic	Low operating pressure and beam current	Wide energy spread
Electron Bombardment	Low Voltage	Wide range of beam current	Low mass utilization
	High Voltage (Canal Ray)		High power and large energy spread
	Crossed Beam	Low energy spread and wide range of beam current	Low beam current
Gas Discharge	Capillary Arc	Monoenergetic	Short life, complicated electronics, hard to stabilize
	Crossed Field (ExB)	High Density	High mass utilization and high proton yield
		Low Density	

Table 2--Mass Separators

Type	Advantages	Disadvantages
Radio Frequency	<ul style="list-style-type: none"> . Handles large beam . Small size . Low total power . Easy intensity adjustment 	<ul style="list-style-type: none"> . $\leq 100\%$ purity . Low transmission of protons . Transmits fast charge exchange neutrals . Must trade beam purity for transmission . Photons from source strike target
Homogeneous Magnetic Field	<ul style="list-style-type: none"> . Pure beam . High transmission . Compatible with scanned beam 	<ul style="list-style-type: none"> . High power for large beam . Energy dispersion
Crossed Field or ExB	<ul style="list-style-type: none"> . Pure beam . Will take large beam 	<ul style="list-style-type: none"> . Two-power supplies . Electric and magnetic aberrations

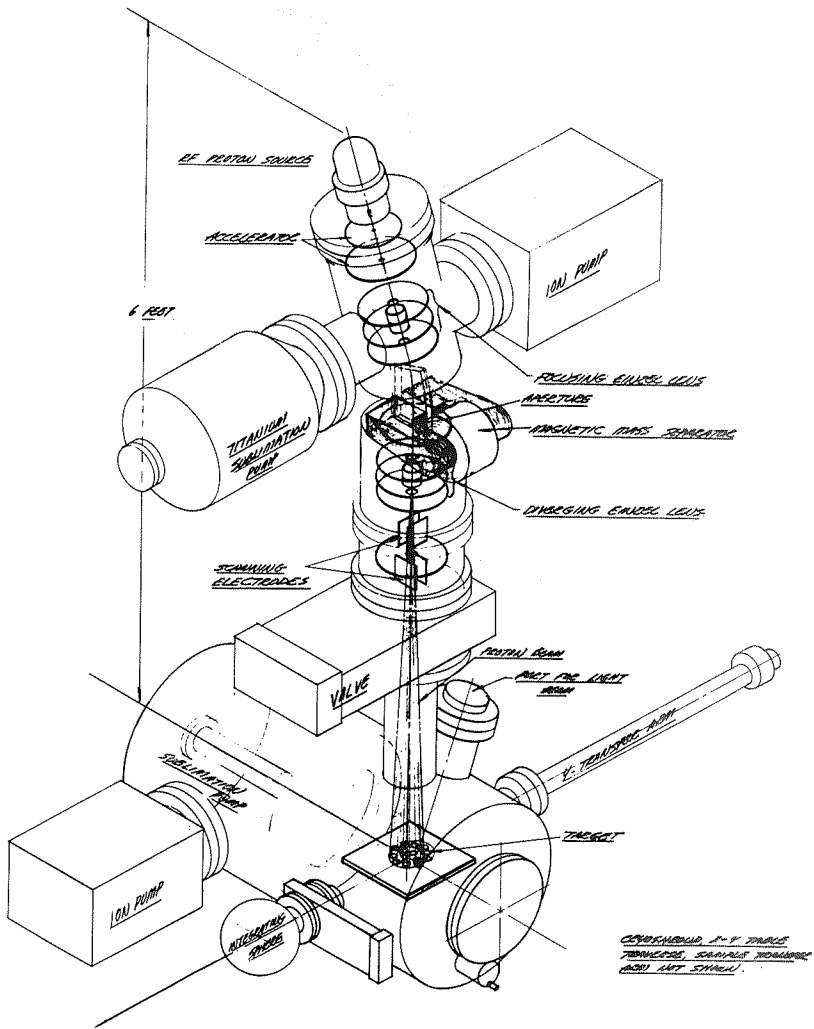
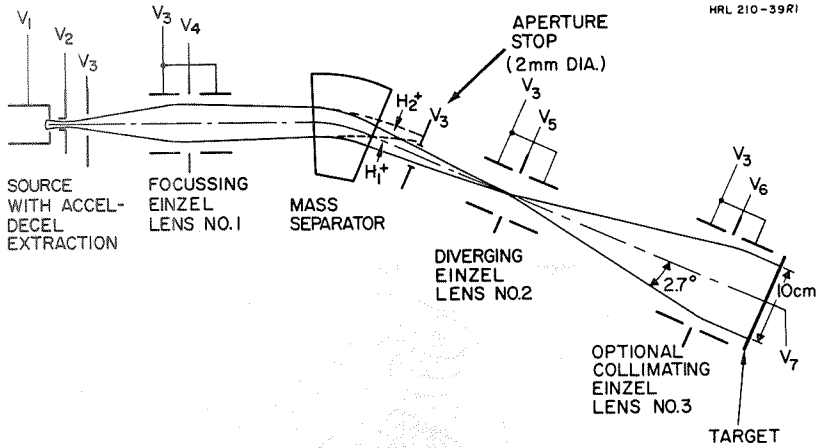


Figure 1--Solar Wind Simulator



Proton Energy	V_1	V_2	V_3	V_4	V_5	V_6	V_7
One Equivalent Sun							
500 v	500	-1250	0	400	465	375	0
1000 v	1000	- 750	0	800	930	750	0
3000 v	3000	- 500	0	2400	2825	2250	0
100 Equivalent Suns ^b							
500 v	500	-1250	0	310	460	375	0
1000 v	1000	- 750	0	605	920	750	0
3000 v	3000	- 500	0	1855	2800	2250	0
^a All voltages measured with respect to ground (target at ground). ^b Source provides additional factor of 10 intensity variation.							

Figure 2--System Schematic

LABORATORY EXPERIMENT ON SOLAR WIND INTERACTION WITH
GEOMAGNETIC FIELD

E.M. Dubinin,¹ G.G. Managadze,¹ I.M. Podgorny¹

It is impossible to reproduce in a laboratory all phenomena which exist at the interaction of the solar wind and the Earth magnetic field. In previous works it was shown that choice of experimental conditions permits one to simulate some of the most interesting effects, for example, the collisionless shock near the Earth magnetosphere. According to the principle of limited simulation, to reproduce the magnetosphere and the collisionless shock the parameters of the artificial solar wind should be:

plasma density - $n = 10^{13} \text{ cm}^{-3}$, electron temperature -
 $T_e = 15 - 20 \text{ ev}$, embedded magnetic field - $B \sim 40 \text{ Oe}$,
ion temperature - $T_i \sim 5 \text{ ev}$, stream velocity - $V =$
 $3 \cdot 10^7 \text{ cm/sec}$.

At these conditions the plasma flux compressed the dipole magnetic field on the day side and formed a configuration of the magnetic field similar to the magnetic field of the Earth tail. Between the artificial magnetosphere and the plasma flow the collisionless shock is displayed. The thickness of the shock is in agreement with plasma theory and has the same order of magnitude in dimensionless expression as in space measurements. In the shock high level magnetic field microfluctuation was discovered. The dimension of the fluctuations is about that of the Larmor radius of ions. The microfluctuations were predicted in plasma theory as a result of Alfvén and magnetosound instability.

In addition to the shock investigations, measurements of the plasma density, velocity and magnetic field strength were carried out before and behind the shock.

KEY WORDS: earth magnetic field, earth tail, magnetosphere, plasma theory, shock wave, solar wind

(Paper not available for publication)

¹Institute for Space Research AN USSR, Moscow, Russia